Mixed-Integer Nonlinear Optimization for District Heating Network Expansion

Marius Roland, Martin Schmidt

Abstract. We present a mixed-integer nonlinear optimization model for computing the optimal expansion of an existing tree-shaped district heating network given a number of potential new consumers. To this end, we state a stationary and nonlinear model of all hydraulic and thermal effects in the pipeline network as well as nonlinear models for consumers and the network's depot. For the former, we consider the Euler momentum and the thermal energy equation. The thermal aspects are especially challenging. Here, we develop a novel polynomial approximation that we use in the optimization model. The expansion decisions are modeled by binary variables for which we derive additional valid inequalities that greatly help to solve the highly challenging problem. Finally, we present a case study in which we identify three major aspects that strongly influence investment decisions: the estimated average power demand of potentially new consumers, the distance between the existing network and the new consumers, and thermal losses in the network.

1. Introduction

Decarbonization and defossilization are at the core of the European energy transition and the European Green Deal, which has been announced at the end of 2019; see, e.g., [7]. Besides measures such as the reduction of CO_2 emissions by coal power plants or a better level of insulation of buildings, the efficient use of the existing energy transport infrastructure is of key importance. The latter aspect can be considered from at least to two different angles. On the one hand, the operation, maintenance, and expansion of energy transport infrastructures such as power or gas networks cost both money and energy and should thus be done in the most efficient way. On the other hand, the consideration of, e.g., the power network, standalone often lead to congestion issues in the recent past, which was more and more governed by highly volatile and uncertain renewable production. This aspect also leads to severe economic implications such as negative electricity prices at the energy exchange in certain days of the year with a high share of renewable energy. The reason is the missing capability of many power systems to store electrical energy or to transform it to other energy forms, i.e., to use power-to-X technologies. At this point, sector coupling enters the scene, which is considered as one of the key technologies towards a successful energy turnaround. Maybe the most intensively discussed sectors to be coupled are gas and electricity, since gas networks itself can be used as large-scale energy storages due to the compressibility of natural gas.

In this paper, we consider another type of energy networks that is not as frequently discussed in the literature: district heating networks. These networks are used to provide households with heat power by a network that transports hot water to the consumers, which is heated usually by waste incineration in a depot. Hence, district

Date: September 15, 2020.

2010 *Mathematics Subject Classification.* 90-XX, 90Cxx, 90C11, 90C35, 90C90.

Key words and phrases. District heating networks, Network expansion, Mixed-integer nonlinear optimization.

heating networks can also be seen as a large-scale energy storage (where energy is stored in terms of thermal energy), e.g., at days with a high renewable share.

To this end, there is a strong need to both operate and extend district heating networks in an optimal way. However, a rigorous mathematical modeling of hydraulic and thermal aspects in district heating networks together with a proper engineering modeling of the depot's processes and consumers leads to highly complex and nonlinear optimization models. Consequently, the literature on the computation of cost-optimal controls of district heating networks mainly uses nonlinear optimization models allowing to accurately describe the physics of the system. However, solving these models over large time horizons induces large computation times. As a remedy, model predictive control approaches are used in [2, 32, 38] to optimally operate the system. In contrast, a highly nonlinear closed-loop model for cost-optimal control of an existing district heating network is presented and solved over long time horizons in [19]. To this end, the authors use different preprocessing and other optimization techniques to reduce computation times.

Besides the optimal control and operation of an existing district heating network, the expansion of existing networks as well as the design of newly built parts are important. Obviously, network expansion is only carried out based on self-interested economic reasoning of the network operator who mainly earns money due to the power consumption of the connected consumers. This network expansion problem is studied in this paper for the special case of tree-shaped networks. We consider an existing district heating network, a set of consumers that are already connected to the network, and another set of potentially new consumers to be given. Based on this data, our model allows to compute the cost-optimal expansion of the network, i.e., the decisions which new consumers should be connected and which new pipes need to be built. Since this decision still depends on the physics in the network, we obtain a nonconvex mixed-integer nonlinear optimization problem (MINLP), which is very challenging to solve.

Mainly two approaches are considered in the related branch of the literature. The most frequently used approach consists in stating the design problem as a mixed-integer linear optimization problem (MILP). This means that all nonlinearities in the system need to be simplified or—at least—linearized to obtain a mixed-integer linear problem, usually at the cost of a significantly larger number of integer variables. Power losses in the system can still be considered, but in a (piecewise) linear fashion. The advantage of the MILP approach is that it usually delivers globally optimal solutions. The models usually incorporate decisions on the layout of the resulting network and on which technologies are installed based on minimizing the total costs of the entire system. These total costs consist of the investment and operational costs, where the latter are based on a cost-optimal control of the system for a set of typical days. Plenty of papers follow this approach and can be further distinguished along the set of technologies that can be installed in the nodes of the system; see, e.g., [1, 6, 36]. Commercial solvers are then usually used to find the optimal solution of the problem. In some cases, the diameter of the pipes is also considered as a decision variable; see, e.g., [29]. Additionally, in some papers, these models are extended towards a multi-objective setting, which allows to minimize the total costs as well as the CO_2 production of the entire system. In [8], this is done using the ε-constraint method and in [26], a genetic algorithm is used. In other papers, the authors also try to reduce the computational complexity by using heuristics to reduce the size of the network [12].

The last papers and the ones discussed in what follows are in contrast to the MILP approach since they do not consider approaches for computing global optima but use heuristics. Genetic algorithms are used as well in the second approach, which

consists in describing the design problem as a mixed-integer nonlinear model [11, 20]. However, these algorithms come with a huge disadvantage because they do not allow for any (sub-)optimality guarantees. Another heuristic technique (however, with a mathematically more solid foundation) is to apply local mixed-integer nonlinear solvers or heuristics are used as, e.g., in [3, 23, 24]. The strength of the mixed-integer nonlinear approach relies on the fact that it allows to include all nonlinearities of the system and thus to have a more accurate description of all power losses.

The papers discussed so far deal with the design problem. In these problems, a completely new district heating network is designed from scratch. In contrast, expansion problems consider an already existing network to be given and ask for an optimal expansion. The expansion of existing district heating systems has been investigated less in the literature. In [4], an MILP is proposed for this problem. No thermal losses are considered and pressure losses are introduced to avoid reaching the pressure bounds of the system. However, pressure losses are not reflected in costs for increasing the pressure in the system.

In the light of the cited papers, our contribution is the following. To the best of our knowledge, we are the first ones who propose a stationary nonconvex mixed-integer nonlinear district heating network expansion model for tree-shaped networks that accurately takes into account pressure losses as well as thermal losses. Let us note that the assumption of a tree-like network is crucial for our modeling of the problem since it significantly reduces the models complexity because flow directions are known in advance and, thus, nonsmooth and highly nonlinear mixing models for the water temperature are not required. The entire model is presented in Section 2, where we also derive some further valid binary inequalities that greatly help to solve the problem. Afterward, in Section 3, we derive a novel polynomial approximation of the solution of the thermal energy equation that we then use in our optimization model. Finally, the model is applied to a realistic test case in Section 4 and we identify the main driving factors that influence investments in new district heating network infrastructure. The paper closes with some concluding remarks and some topics of future research in Section 5.

2. Problem Statement

In this section, we present a model for optimal district heating network expansion. The model makes it possible to decide if it is economically reasonable to connect potential new consumers to an existing district heating network that is assumed to be tree-shaped. We distinguish between investment decisions (i.e., which pipes and consumers should be connected to the existing network) and operational decisions for controlling the network. To keep the resulting problem tractable, we restrict ourselves to the stationary setting. This can be seen as that the investment decisions are taken up-front and that the computed operational decisions are optimal for the expanded network. Obviously, investment decisions influence operational decisions and vice versa.

First, we introduce the graph describing the already existing network as well as the potential new consumers and pipes that can be added to the network. Then, the constraints of the optimization problem are presented, followed by the objective function and an overall model summary.

2.1. **Network Topology.**

To describe the topology of a district heating network, we first discuss the relevant network elements and the corresponding arc set A and and node set V of the underlying directed and connected graph $G = (V, A)$. To this end, we mainly follow the notation introduced in [19] and extend it. A typical district heating network consists of the following parts:

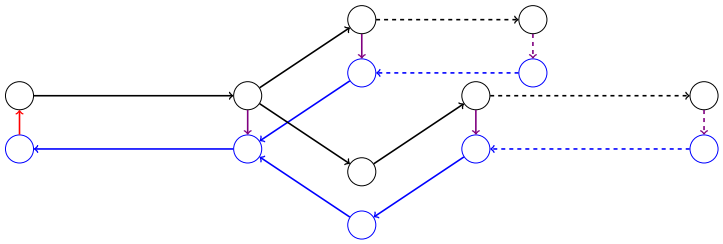

FIGURE 1. Schematic illustration of a district heating network. Black arcs and nodes represent pipes in A_{ff} and nodes in V_{ff}. Blue arcs and nodes represent pipes in A_{bf} and nodes in V_{bf}. Purple arcs are consumers in A_{c} and the red arc is the depot a_{d}. Overall, solid arcs represent existing arcs in $A^{\mathrm{e}}_{\mathrm{ff}} \cup A^{\mathrm{e}}_{\mathrm{bf}} \cup A^{\mathrm{e}}_{\mathrm{c}}$, whereas dashed arcs represent for candidate arcs in $A^{\mathrm{c}}_{\mathrm{ff}} \cup A^{\mathrm{c}}_{\mathrm{bf}} \cup A^{\mathrm{c}}_{\mathrm{c}}$.

(i) A depot $a_{\mathrm{d}} \in A$ at which the water is heated to satisfy the energy demand of the connected consumers. Moreover, the pressure is increased to propel the water flow in the network.
(ii) Consumers $a \in A_{\mathrm{c}} \subset A$ that extract energy from the hot water circulating in the network.
(iii) A forward-flow part consisting of pipes $a \in A_{\mathrm{ff}}$, which are used to transport the heated water from the depot to the consumers. The node set V_{ff} represents the nodes in the forward-flow part of the network. These nodes serve as intersections between the depot and adjacent consumers and pipes.
(iv) A backward-flow part consisting of pipes $a \in A_{\mathrm{bf}}$, which transport the cooled water from consumers back to the depot. The node set V_{bf} represents the nodes in the backward-flow part of the network as it is the case for the forward-flow network.

In particular, consumers are always of the type $a \in A_{\mathrm{c}}$ with $a = (u, v)$ and $u \in V_{\mathrm{ff}}$, $v \in V_{\mathrm{bf}}$. Contrarily, the single depot of the network is of type $a_{\mathrm{d}} = (u_{\mathrm{d}}, v_{\mathrm{d}})$ with $u_{\mathrm{d}} \in V_{\mathrm{bf}}$ and $v_{\mathrm{d}} \in V_{\mathrm{ff}}$. With these notations at hand, we have

$$A = \{a_{\mathrm{d}}\} \cup A_{\mathrm{c}} \cup A_{\mathrm{ff}} \cup A_{\mathrm{bf}}, \quad V = V_{\mathrm{ff}} \cup V_{\mathrm{bf}}.$$

Moreover, the set of consumers A_{c} is split up into already connected consumers $a \in A^{\mathrm{e}}_{\mathrm{c}}$ and potential new, i.e., candidate, consumers $a \in A^{\mathrm{c}}_{\mathrm{c}}$. Thus, we have $A_{\mathrm{c}} = A^{\mathrm{e}}_{\mathrm{c}} \cup A^{\mathrm{c}}_{\mathrm{c}}$. Other existing network elements are also super-indexed with "e", whereas potential new, i.e., candidate, elements are super-indexed with "c". Consequently, we also have $A_{\mathrm{ff}} = A^{\mathrm{e}}_{\mathrm{ff}} \cup A^{\mathrm{c}}_{\mathrm{ff}}$ and $A_{\mathrm{bf}} = A^{\mathrm{e}}_{\mathrm{bf}} \cup A^{\mathrm{c}}_{\mathrm{bf}}$ as well as $V_{\mathrm{ff}} = V^{\mathrm{e}}_{\mathrm{ff}} \cup V^{\mathrm{c}}_{\mathrm{ff}}$ and $V_{\mathrm{bf}} = V^{\mathrm{e}}_{\mathrm{bf}} \cup V^{\mathrm{c}}_{\mathrm{bf}}$.

As already discussed in the introduction, we restrict ourselves to the case in which the district heating network is tree-shaped. In this context, a tree-shaped district heating network is a graph for which both the forward and the backward flow part standalone are trees, i.e., directed acyclic graphs. To be more specific, the forward flow part of the network is a rooted out-tree and the backward flow part is a rooted in-tree, where the root is depot of the network. Note, however, that the entire network always contains cycles since the forward and backward flow parts are connected via the depot and the consumers. Table 1 summarizes the graph notation and Figure 1 shows an exemplary district heating network with additional candidate consumers and pipes.

2.2. **Existing Pipes.** In this section, we describe the modeling of all pipes that are already existing in the network, i.e., of all arcs $a = (u, v) \in A^{\mathrm{e}}_{\mathrm{ff}} \cup A^{\mathrm{e}}_{\mathrm{bf}}$. First, we

TABLE 1. Arc and node sets.

Symbol	Description
a_{d}	Depot
A_{c}	Consumers
$A_{\mathrm{c}}^{\mathrm{e}} \subset A_{\mathrm{c}}$	Existing consumers
$A_{\mathrm{c}}^{\mathrm{c}} \subset A_{\mathrm{c}}$	Candidate consumers
A_{ff}	Pipes in the forward-flow network
$A_{\mathrm{ff}}^{\mathrm{e}} \subset A_{\mathrm{ff}}$	Existing pipes in the forward-flow network
$A_{\mathrm{ff}}^{\mathrm{c}} \subset A_{\mathrm{ff}}$	Candidate pipes in the forward-flow network
A_{bf}	Pipes in the backward-flow network
$A_{\mathrm{bf}}^{\mathrm{e}} \subset A_{\mathrm{bf}}$	Existing pipes in the backward-flow network
$A_{\mathrm{bf}}^{\mathrm{c}} \subset A_{\mathrm{bf}}$	Candidate pipes in the backward-flow network
V_{ff}	Nodes in the forward-flow network
$V_{\mathrm{ff}}^{\mathrm{e}} \subset V_{\mathrm{ff}}$	Existing nodes in the forward-flow network
$V_{\mathrm{ff}}^{\mathrm{c}} \subset V_{\mathrm{ff}}$	Candidate nodes in the forward-flow network
V_{bf}	Nodes in the backward-flow network
$V_{\mathrm{bf}}^{\mathrm{e}} \subset V_{\mathrm{bf}}$	Existing nodes in the backward-flow network
$V_{\mathrm{bf}}^{\mathrm{c}} \subset V_{\mathrm{bf}}$	Candidate nodes in the backward-flow network

derive the required equations to model the hot water flow in the network; see, e.g., [5, 18, 31]. Note that these equations are very similar to the Euler equations that are typically used for natural gas network optimization; see, e.g., [9, 33, 34]. To this end, let L_a denote the length of pipe a and let $x \in [0, L_a]$ be the spatial position in the pipe. For the ease of presentation and since we are only considering the stationary case in this paper, we directly state the stationary variants of the corresponding nonlinear partial differential equations. The one-dimensional stationary continuity equation for compressible fluids in cylindrical pipes is given by

$$\frac{\mathrm{d}(\rho_a v_a)}{\mathrm{d}x} = 0, \tag{1}$$

where $\rho_a(\cdot)$ and $v_a(\cdot)$ denote the density and the velocity of the water depending on the spatial position in the pipe, respectively; see e.g., [17, 19] for the instationary setting. Obviously, Equation (1) is equivalent to

$$\rho_a \frac{\mathrm{d}v_a}{\mathrm{d}x} + v_a \frac{\mathrm{d}\rho_a}{\mathrm{d}x} = 0.$$

Using the incompressibility of water, which is modeled via

$$v_a \frac{\mathrm{d}\rho_a}{\mathrm{d}x} = 0,$$

see, e.g., [21], we see that Equation (1) reads

$$\rho_a \frac{\mathrm{d}v_a}{\mathrm{d}x} = 0$$

in the incompressible case. Since $\rho_a(x) > 0$ for all x, we finally obtain

$$\frac{\mathrm{d}v_a}{\mathrm{d}x} = 0, \tag{2}$$

which implies that velocity $v_a(x) = v_a$ is constant in a pipe.

Next, we consider the one-dimensional stationary momentum equation for compressible fluids in cylindrical pipes, which is given by the nonlinear differential

equation

$$\frac{\mathrm{d}p_a}{\mathrm{d}x} + \frac{\mathrm{d}(\rho_a v_a^2)}{\mathrm{d}x} + g\rho_a h_a' + \lambda_a \frac{|v_a| v_a \rho_a}{2D_a} = 0;$$

see again [17, 19] for the instationary setting. The function p_a represents the water pressure at the spatial position x and g, h_a', and D_a represent gravitational acceleration, the pipe's slope, and the inner diameter of pipe a, respectively. Friction λ_a at the rough inner pipe wall is modeled using the law of Nikuradse [5], i.e.,

$$\lambda_a = \left(2\log_{10}\left(\frac{D_a}{k_a}\right) + 1.138\right)^{-2},$$

where k_a is the roughness of the inner pipe's wall. Incompressibility and (2) imply

$$\frac{\mathrm{d}(\rho_a v_a^2)}{\mathrm{d}x} = 0,$$

which yields

$$\frac{\mathrm{d}p_a}{\mathrm{d}x} = -g\rho_a h_a' - \lambda_a \frac{|v_a| v_a \rho}{2D_a}. \tag{3}$$

The additional assumption that the density $\rho_a(x) = \rho_a = \rho$ is constant in the entire network leads to a right-hand side in (3) that is independent of x. Thus, the pressure $p_a(x)$ is linear in x, which leads to the momentum equation

$$\frac{p_a(L_a) - p_a(0)}{L_a} = -g\rho h_a' - \lambda_a \frac{|v_a| v_a \rho}{2D_a}, \tag{4}$$

where L_a denotes the length of pipe a.

Next, we describe the thermal behavior of water flow in the pipe using the one-dimensional stationary thermal energy equation

$$v_a \frac{\mathrm{d}T_a}{\mathrm{d}x} + \frac{4U_a}{c_\mathrm{p}\rho D_a}(T_a - T_\mathrm{soil}) = 0; \tag{5}$$

see again [17, 19] for the instationary setting. Here and in what follows, water temperature at the spatial position x is denoted with $T_a(x)$ and the parameters U_a, c_p, and T_soil represent the heat transfer coefficient of the pipe's wall, the specific heat capacity of water, and the temperature of the surrounding soil of the pipe, respectively. Equation (5) is a first-order ordinary differential equation (ODE) and can be solved as stated in the following lemma. To simplify the presentation let us remark that both water flows as well as velocities can be assumed to be nonnegative since the network is a tree and we have only a single depot.

Lemma 1. *The ODE (5),*

$$v_a \frac{\mathrm{d}T_a}{\mathrm{d}x}(x) + \frac{4U_a}{c_\mathrm{p}\rho D_a}(T_a(x) - T_{soil}) = 0,$$

has the solution

$$T_a(x; v_a) = \begin{cases} T_{soil}, & \text{if } v_a = 0, \\ Ce^{-\frac{4U_a x}{c_\mathrm{p}\rho D_a v_a}} + T_{soil}, & \text{if } v_a > 0, \end{cases} \tag{6}$$

where $C \in \mathbb{R}$ is a constant. The solution is continuous for all $x \in [0, L_a]$ and all $v_a \geq 0$.

The proof of this lemma is rather straightforward and can be found in Appendix A.

For a macroscopic network modeling, we are again mainly interested in the relation between the quantities at the end nodes of the pipes as it is also the case for the pressure loss equation (4) that couples inflow and outflow pressure as well as the water flow on the arc. Regarding the temperature loss model, we aim for something similar but for a coupling of inflow and outflow temperature as well as

the flow on the arc. As usual, the constant C appears in the general solution of the stationary thermal energy equation as given in Lemma 1. If the latter ODE is considered as an initial value problem with the initial value being the inflow water temperature, this constant can be specified in dependence of the initial value, i.e.,

$$T_a(0; v_a) = C + T_{\text{soil}}$$

holds for $v_a > 0$. This means that the constant represents the offset between the inflow and the soil temperature. Going further, we can rewrite the solution as

$$T_a(L_a; v_a) = \begin{cases} T_{\text{soil}}, & v_a = 0, \\ (T_a(0) - T_{\text{soil}})\, e^{-\frac{4U_a L_a}{c_p \rho D_a v_a}} + T_{\text{soil}}, & v_a > 0. \end{cases} \tag{7}$$

It is easy to see that $T_a(L_a; v_a)$ is smooth at $v_a = 0$. However, the problem is that this function is defined by a case distinction ($v_a = 0$ vs. $v_a \neq 0$) since the second part of the function's definition is not defined for $v_a = 0$. This renders the integration of (7) into a model that should later be solved by a global MINLP solver impossible. Furthermore, it is not possible to simply include the second part of the definition standalone in the model since the resulting constraint would not be well-defined in all cases in which an arc has a zero flow, which is, e.g., the case for all candidate pipes that are not built. To tackle this problem, we will derive an approximation f_{approx} in Section 3 so that (7) is approximately captured via using the equality constraint $f_{\text{approx}} = 0$.

Finally note that all physical equations in this section are stated using the velocity v_a of the water flow in the pipe. Using the formula $q_a = \rho A_a v_a$ with $A_a = \pi(D_a/2)^2$, which directly connects velocity v_a with the mass flow q_a (note again that ρ is constant), we can also state all equations such as the momentum or the thermal energy equation in terms of mass flow instead of velocity.

2.3. **Nodes.** Nodes are used to connect adjacent pipes or other types of arcs. At nodes, we need to model three different phenomena:

(i) mass conservation,
(ii) pressure continuity, and
(iii) mixing of different inflowing water temperatures.

For stating mass conservation, we introduce the notations

$$\delta^{\text{in}}(u) := \{a \in A \colon \exists v \in V \text{ with } a = (v, u)\},$$
$$\delta^{\text{out}}(u) := \{a \in A \colon \exists v \in V \text{ with } a = (u, v)\}$$

for incoming and outgoing arcs at node $u \in V$. With this, the mass flow q_a needs to satisfy

$$\sum_{a \in \delta^{\text{in}}(u)} q_a = \sum_{a \in \delta^{\text{out}}(u)} q_a, \quad u \in V. \tag{8}$$

Pressure continuity at nodes is easily modeled using

$$\begin{aligned} p_u &= p_a(0), \quad u \in V,\ a \in \delta^{\text{out}}(u), \\ p_u &= p_a(L_a), \quad u \in V,\ a \in \delta^{\text{in}}(u), \end{aligned} \tag{9}$$

where p_u is the pressure at node u.

Finally, we need to model the mixing of different inflowing water temperatures at a node of the network. In [19], a formulation of the required nodal mixing constraints has been introduced for general district heating networks, which is based on analogous models for natural gas networks; see, e.g., [10, 14, 35]. In general network structures, which can also contain cycles, the directions of water flow are not known in advance. This leads to nonsmooth constraints that introduce significant additional hardness to the overall problem. Due to our simplifying assumption

of only considering tree-shaped networks (i.e., the graphs of the forward and the backward-flow part of the network are trees), we can fix the direction of the flow in the pipes in advance. This is explained by the fact that a consumer cannot obtain water if the flow direction in a pipe on the unique path from the depot to the consumer changes. The same applies for the backward-flow part but in the opposite direction. This also implies that we can w.l.o.g. assume that all mass flows in the network are positive. Thus, the model introduced in [19] specifies to

$$T_u = \frac{\sum_{a\in\delta^{\mathrm{in}}(u)} c_{\mathrm{p}} q_a T_{a,\mathrm{out}}}{\sum_{a\in\delta^{\mathrm{in}}(u)} c_{\mathrm{p}} q_a}, \quad u \in V, \tag{10a}$$

$$T_u = T_a(0), \quad u \in V,\ a \in \delta^{\mathrm{out}}(u). \tag{10b}$$

Here, $T_{a,\mathrm{out}}$ stands for the water temperature at the outlet of arc a. For pipes, this corresponds to $T_a(L_a)$. Equation (10a) is obtained by using the law of conservation of energy. If c_{p} is a constant throughout the network and the same for all pipes, we finally obtain

$$T_u = \frac{\sum_{a\in\delta^{\mathrm{in}}(u)} q_a T_{a,\mathrm{out}}}{\sum_{a\in\delta^{\mathrm{in}}(u)} q_a}, \quad u \in V,$$

$$T_u = T_a(0), \quad u \in V,\ a \in \delta^{\mathrm{out}}(u).$$

2.4. **Depot and Consumers.** We now state the constraints modeling the depot and the consumers. For the depot $a_{\mathrm{d}} = (u_{\mathrm{d}}, v_{\mathrm{d}})$ we have,

$$p_{u_{\mathrm{d}}} = p_{\mathrm{s}}, \tag{11a}$$

$$P_{\mathrm{p}} = \frac{q_{a_{\mathrm{d}}}}{\rho}\left(p_{v_{\mathrm{d}}} - p_{u_{\mathrm{d}}}\right), \tag{11b}$$

$$P_{\mathrm{w}} + P_{\mathrm{g}} = q_{a_{\mathrm{d}}} c_{\mathrm{p}}\left(T_{a,\mathrm{out}} - T_{a,\mathrm{in}}\right). \tag{11c}$$

Here, $T_{a,\mathrm{in}}$ and $T_{a,\mathrm{out}}$ represent the inflow and outflow water temperature at the depot. Moreover, p_{s} stands for the stagnation pressure. The stagnation pressure, to which the depot's inflow pressure is set, leads to pressure values in the entire network that are uniquely determined by the pressure loss constraints (4). The variables P_{p}, P_{w}, and P_{g} stand for the power needed to increase the water pressure, the power used for heating the water obtained by waste incineration, and the power produced by burning natural gas. As one can see, power consumption mainly depends on the products of temperature or pressure differences and the mass flow.

The constraints modeling consumers $a = (u, v)$ read

$$P_a = q_a c_{\mathrm{p}}\left(T_{a,\mathrm{out}} - T_{a,\mathrm{in}}\right), \qquad a \in A_{\mathrm{c}}^{\mathrm{e}}, \tag{12a}$$

$$x_a P_a = q_a c_{\mathrm{p}}\left(T_{a,\mathrm{out}} - T_{a,\mathrm{in}}\right), \qquad a \in A_{\mathrm{c}}^{\mathrm{c}}, \tag{12b}$$

$$T_{a,\mathrm{out}} = T^{\mathrm{bf}}, \qquad a \in A_{\mathrm{c}}, \tag{12c}$$

$$T_{a,\mathrm{in}} \geq T_a^{\mathrm{ff}}, \qquad a \in A_{\mathrm{c}}, \tag{12d}$$

$$p_v \leq p_u, \qquad a \in A_{\mathrm{c}}. \tag{12e}$$

In (12a) and (12b), the parameter P_a stands for the average power demand of the consumer. Additionally, the binary variable $x_a \in \{0, 1\}$ is introduced for deciding if arc $a \in A_{\mathrm{c}}^{\mathrm{c}}$ is connected or not. We show in Section 2.5 that x_a is also used to force a zero mass flow in arc a if the decision is made to not connect a ($x_a = 0$). Since in this case, the right-hand side of (12b) is zero, we multiply the left-hand side by x_a to ensure the validity of the constraint. The parameter T^{bf} is the consumer's outlet water temperature and is the same for all consumers. The parameter T_a^{ff} represents the contractually fixed lower bound of the consumer's inflow temperature.

Finally, Constraint (12e) implies that the outlet pressure of the consumer is not greater than its inlet pressure.

2.5. **Bounds.** We now introduce bounds on the variables of our model and make a distinction between existing and candidate arcs if needed. First, we state the bounds on mass flow,

$$0 \leq q_a \leq q_a^+, \qquad a \in A_{\mathrm{ff}}^{\mathrm{e}} \cup A_{\mathrm{bf}}^{\mathrm{e}} \cup A_{\mathrm{c}}^{\mathrm{e}}, \tag{13a}$$

$$0 \leq q_a \leq x_a q_a^+, \qquad a \in A_{\mathrm{ff}}^{\mathrm{c}} \cup A_{\mathrm{bf}}^{\mathrm{c}} \cup A_{\mathrm{c}}^{\mathrm{c}}, \tag{13b}$$

where the parameters q_a^+ define upper bounds on the mass flow and are usually imposed for avoiding pipe damages as well as excessive noise emissions. In the latter constraint we again use the binary variables $x_a \in \{0,1\}$ for all possibly built arcs $a \in A_{\mathrm{ff}}^{\mathrm{c}} \cup A_{\mathrm{bf}}^{\mathrm{c}} \cup A_{\mathrm{c}}^{\mathrm{c}}$. Thus, this constraint obviously enforces $q_a = 0$ for $a \in A^{\mathrm{c}}$ if $x_a = 0$; cf. (12b). Note also that this immediately implies $v_a = 0$ as well. Next, we introduce bounds on the nodal pressure variables

$$0 \leq p_u \leq p_u^+, \quad u \in V. \tag{14}$$

Moreover, we have bounds on the nodal water temperature, i.e.,

$$T_u \in [T_u^-, T_u^+], \quad u \in V. \tag{15}$$

Finally, we incorporate bounds on the power consumption, i.e.,

$$P_{\mathrm{p}} \in [0, P_{\mathrm{p}}^+], \quad P_{\mathrm{w}} \in [0, P_{\mathrm{w}}^+], \quad P_{\mathrm{g}} \in [0, P_{\mathrm{g}}^+]. \tag{16}$$

2.6. **Candidate Pipes.** For candidate pipes, we need to make some adaptions to the equations presented in Section 2.2. For existing pipes, the hydraulic effects are modeled using (4), i.e.,

$$p_v - p_u + L_a g \rho h'_a + \lambda_a \frac{|v_a| v_a \rho L_a}{2 D_a} = 0,$$

and by the constraint $f_{\mathrm{approx}} = 0$ as discussed at the end of the Section 2.2. Obviously, both constraints need to be present if a candidate pipe $a = (u, v) \in A_{\mathrm{ff}}^{\mathrm{c}} \cup A_{\mathrm{bf}}^{\mathrm{c}}$ is decided to be installed. However, if the pipe is not built, these constraints need to be de-activated. To this end, we introduce a binary variable $x_a \in \{0,1\}$ for every candidate pipe with $x_a = 0$ if the pipe is not built and $x_a = 1$ if it is built. With this decision variable at hand, we then restate the momentum equation as

$$p_v - p_u + L_a g \rho h'_a + \lambda_a \frac{|v_a| v_a \rho L_a}{2 D_a} \leq (1 - x_a) M_a^1, \tag{17a}$$

$$p_v - p_u + L_a g \rho h'_a + \lambda_a \frac{|v_a| v_a \rho L_a}{2 D_a} \geq -(1 - x_a) M_a^2 \tag{17b}$$

with suitably large constants M_a^1, M_a^2 that can be chosen as

$$M_a^1 = p_v^+ - p_u^- + L_a g \rho h'_a,$$
$$M_a^2 = p_v^- - p_u^+ + L_a g \rho h'_a.$$

Note that the friction part of the momentum equation (4) can be ignored due to the implied bounds in (13b). Interestingly, an analogous big-M formulation is not required for the approximation of the thermal energy equation; see Section 3.

2.7. **Valid Inequalities for Candidate Arcs.** In this section, we briefly derive valid inequalities for the binary expansion decision variables of the model. These additional inequalities are not required to obtain a correct model but we will later show that they greatly help global solvers to solve the problem.

We split the description of the inequalities into three cases and start with a candidate pipe $a \in A^{\mathrm{c}}_{\mathrm{ff}}$ in the forward-flow part of the network. Let $P(a) \subseteq A^{\mathrm{c}}_{\mathrm{ff}}$ be the set of arcs of the path connecting a to the existing forward-flow network. This path is unique since we consider tree-shaped networks. The valid additional constraints

$$x_a \leq x_{\bar{a}}, \quad \bar{a} \in P(a), \tag{18}$$

then model that all pipes on the way from the existing forward-flow part of the network to the newly built pipe also need to be built.

For a candidate pipe $a \in A^{\mathrm{c}}_{\mathrm{bf}}$ in the backward-flow part of the network, the idea and the valid inequalities are the same. The only difference is that the arcs in the path $P(a)$ are now part of the backward-flow network and are oriented in the other direction compared to the path in the forward-flow network.

Third and finally, if $a = (u, v) \in A^{\mathrm{c}}_{\mathrm{c}}$ is a potential new consumer, we combine both ideas and introduce (18) for the forward-flow part of the network (using the path that connects the consumer's inlet node $u \in V_{\mathrm{ff}}$ with the existing forward-flow part of the network) as well as for the backward-flow part of the network (using the path that connects the consumer's outlet node $v \in V_{\mathrm{bf}}$ with the existing backward-flow part of the network).

2.8. **Objective Function.** The objective function to maximize reads

$$\sum_{a \in A^{\mathrm{c}}_{\mathrm{c}}} P_a w \pi x_a - \sum_{a \in A^{\mathrm{c}}} C^{\mathrm{inv}}_a x_a - w \left(C_{\mathrm{p}} P_{\mathrm{p}} + C_{\mathrm{w}} P_{\mathrm{w}} + C_{\mathrm{g}} P_{\mathrm{g}} \right), \tag{19}$$

where $w = 24$ and π, C^{inv}_a, C_{p}, C_{w}, and C_{g} stand for the energy price per kWh, the daily annuity costs of arc a, the price per pressure increase (measured in kWh), the price of energy from waste incineration per kWh, and the price of energy from gas per kWh, respectively. The first part of the objective, corresponding to the candidate consumer payments, models how much a new consumer pays in average over a day if connected to the network. The second part, which corresponds to investment costs, represents how much is paid per day in order to install arc $a \in A^{\mathrm{c}}$. The last part, corresponding to the power cost, represents how much the network operator pays to satisfy the energy demand of the possibly extended district heating system. Here, we abstract from operation and maintenance costs.

2.9. **Model Summary.** For later reference, we now finally state the complete optimization problem for computing the optimal investments to connect new consumers

TABLE 2. Variables of Problem (20)

Variable	Index Set
$P_\mathrm{p}, P_\mathrm{w}, P_\mathrm{g}$	—
x_a	$a \in A_\mathrm{ff}^\mathrm{c} \cup A_\mathrm{bf}^\mathrm{c} \cup A_\mathrm{c}^\mathrm{c}$
v_a	$a \in A_\mathrm{ff} \cup A_\mathrm{bf}$
q_a	$a \in A_\mathrm{ff} \cup A_\mathrm{bf} \cup A_\mathrm{c} \cup \{a_\mathrm{d}\}$
p_u, T_u	$u \in V$
$p_a(0), p_a(L_a)$	$a \in A_\mathrm{ff} \cup A_\mathrm{bf}$
$T_{a,\mathrm{in}}, T_{a,\mathrm{out}}$ (resp. $T_a(0), T_a(L_a)$)	$a \in A$

to an existing district heating network:

$$\begin{aligned}
\max \quad & \text{objective (19)}, && \text{(20a)}\\
\text{s.t.} \quad & \text{stationary incompressible Euler equation (4) or (17)}, && \text{(20b)}\\
& \text{stationary thermal energy equation (7)}, && \text{(20c)}\\
& \text{mass conservation (8)}, && \text{(20d)}\\
& \text{pressure continuity (9)}, && \text{(20e)}\\
& \text{temperature mixing equations (10)}, && \text{(20f)}\\
& \text{depot constraints (11)}, && \text{(20g)}\\
& \text{consumer constraints (12)}, && \text{(20h)}\\
& \text{mass flow bounds (13)}, && \text{(20i)}\\
& \text{pressure bounds (14)}, && \text{(20j)}\\
& \text{temperature bounds (15)}, && \text{(20k)}\\
& \text{power bounds (16)}, && \text{(20l)}\\
& \text{valid binary inequalities (18)}. && \text{(20m)}
\end{aligned}$$

All variables are listed in Table 2.

3. Approximation of the Thermal Energy Equation

We now deduce the approximation of the solution of the thermal energy equation for all pipes $a = (u, v) \in A_\mathrm{ff} \cup A_\mathrm{bf}$. As already mentioned in Section 2.2, the main goal is to obtain a constraint using a single symbolic expression (instead of the case distinction in (7)) so that inflow and outflow water temperature of a pipe are coupled to the water flow through the pipe as given in (7). To this end, we define the function $f(v_a, T_a(0), T_a(L_a))$, which depends on the three discussed physical quantities, based on Equation (7) as

$$f(v_a, T_a(0), T_a(L_a)) := \begin{cases} \big(T_a(0) - T_\mathrm{soil}\big) e^{-\frac{4U_a L_a}{c_\mathrm{p} \rho D_a v_a}} + T_\mathrm{soil} - T_a(L_a), & v_a > 0, \\ T_\mathrm{soil} - T_a(L_a), & v_a = 0. \end{cases}$$

Ideally, we would like to incorporate the constraint $f(v_a, T_a(0), T_a(L_a)) = 0$ that couples the inlet and outlet temperature of a pipe with the velocity of hot water flow in our model. However, this is not possible directly due to the function f being defined via a case distinction. Thus, we design a continuous ansatz function $f_\mathrm{approx}(v_a, T_a(0), T_a(L_a))$ satisfying the following conditions:

(i) If $v_a = 0$, then $f_\mathrm{approx}(v_a, T_a(0), T_a(L_a)) = 0$ reduces to $T_a(L_a) = T_\mathrm{soil}$.

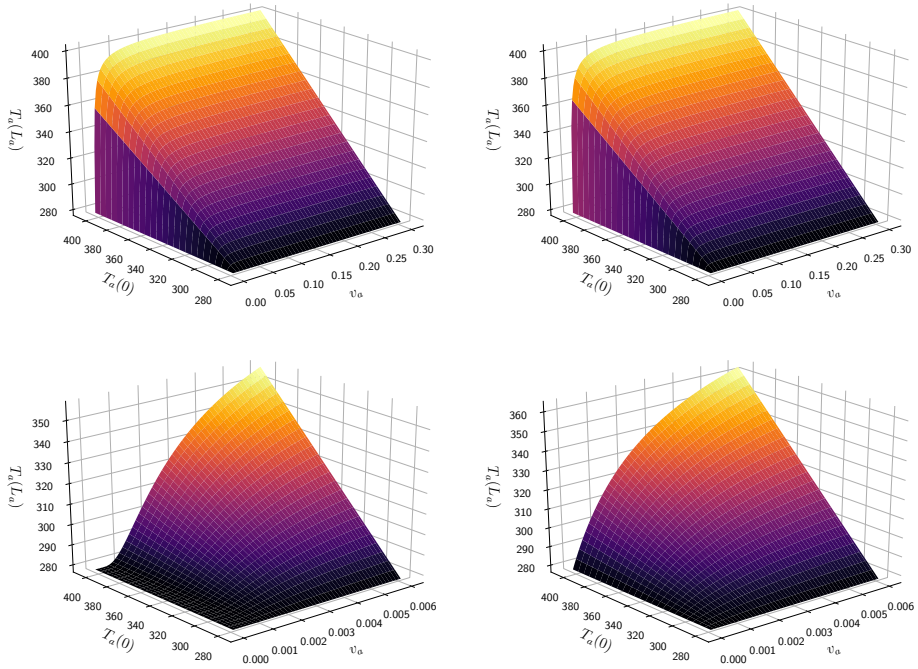

FIGURE 2. Solution of the thermal energy equation (left figures) and its degree-2 polynomial approximation (right figures) for $U_a = 0.5\,\mathrm{W\,m^{-2}\,K^{-1}}$, $c_\mathrm{p} = 4181.3\,\mathrm{J\,kg^{-1}\,K^{-1}}$, $\rho_a = 1000\,\mathrm{kg\,m^{-3}}$, $D_a = 0.07\,\mathrm{m}$, $L_a = 400\,\mathrm{m}$, and $T_\mathrm{soil} = 278\,\mathrm{K}$. For larger values of v_a (top figures) the approximation is nearly identical to the original thermal energy equation solution. Whereas the approximation does not possess similar curvature for values of v_a close to 0 (bottom figures).

(ii) The approximation f_approx is continuous and as close as possible to 0 for all reasonable combinations of $v_a \in [0, v_a^+]$ and $T_a(0), T_a(L_a) \in [T_v^-, T_v^+]$ that satisfy the thermal energy equation.

The main rationale is to use a polynomial of degree d as the ansatz function, i.e.,

$$f_\mathrm{approx}(v_a, T_a(0), T_a(L_a)) = \sum_{(k,l,m)\in\Gamma_d} \alpha_{klm}\, v_a^k\, T_a(0)^l\, T_a(L_a)^m,$$

with coefficients α_{klm} and

$$\Gamma_d := \left\{(k,l,m) \in \mathbb{N}^3 \colon k + l + m \le d\right\}.$$

However, it is reasonable to slightly modify this ansatz and to replace it with

$$f_\mathrm{approx}(v_a, T_a(0), T_a(L_a)) = \sum_{(k,l,m)\in\Theta_d} \alpha_{klm}\, v_a^k\, T_a(0)^l\, T_a(L_a)^m + T_a(L_a) - T_\mathrm{soil} \quad (21)$$

and

$$\Theta_d := \left\{(k,l,m) \in \mathbb{N}^3 \colon k \neq 0 \text{ and } k + l + m \le d\right\}.$$

By doing so, the Condition (i) above is always satisfied by construction. Let us also note that Condition (i) is sufficient to exclude the trivial solution $\alpha_{klm} = 0$ for all $(k,l,m) \in \Theta_d$. To satisfy the Condition (ii) we compute the polynomial's

coefficients α_{klm} in (21) using the least-squares fit

$$\min_{\alpha} \quad \sum_{i \in I} f_{\text{approx}}(v_a^i, T_a(0)^i, T_a(L_a)^i)^2.$$

For our computations, we use a large number of equidistant vectors

$$(v_a, T_a(0)) \in [0, v_a^+] \times [T_v^-, T_v^+]$$

and compute the corresponding outlet temperature $T_a(L_a)$ by solving the thermal energy equation. The resulting vectors in $\mathbb{R}^3$ then form the set I for the least-squares fit.

Figure 2 shows the degree-2 approximation for a certain pipe. One can see that the approximation is pretty accurate. However, for positive values of v_a very close to zero the approximation is not able to reflect the curvature of the original thermal energy equation.

We close this section with a discussion of the introduced approximation of the solution of the stationary thermal energy equation in the context of candidate pipes. In Section 2.6, we explicitly reformulated the momentum equation for candidate pipes. This is not required for the approximation of the thermal energy equation's solution since we can always include the corresponding constraint as it is—independent of whether the candidate pipe is built or not. The reason is as follows. If a candidate pipe is not built, the constraints in (13) force the velocity, and thus the mass flow, to zero. However, in this case, $f_{\text{approx}}(0, T_a(0), T_a(L_a)) = 0$ implies $T_a(L_a) = T_{\text{soil}}$; see (21). Since $T_{\text{soil}} \in [T_u^-, T_u^+]$ always holds, no adaptions are required for the thermal modeling on candidate pipes.

To conclude, the final model is given by Problem (20) with Constraint (7) replaced by $f_{\text{approx}}(0, T_a(0), T_a(L_a)) = 0$ for every pipe $a \in A_{\text{ff}} \cup A_{\text{bf}}$.

4. Numerical Results

In this section, we first describe the software and hardware setup that we use for our numerical tests, then present a basic test case, and discuss its numerical results. Afterward, we slightly modify the network's setup to carry out a sensitivity analysis that allows to conclude on the key decision parameters for optimal district heating network expansion. To the best of our knowledge, we are the first to consider a district heating network expansion problem equipped with the level of physical and technical detail as discussed in this paper. Thus, the aim of the following discussion of the numerical results is to showcase the impact of certain key aspects on the expansion decisions. This means that we try to answer the question on what the governing factors for expansions are if an accurate nonlinear physics model is used. To this end, we choose a network size that is non-trivial but that still allows to discuss the physical and investment solution in detail for different parameterizations of the problem at hand.

4.1. **Software and Hardware Setup.** We implemented the model in Python v.3.7.4 using the Pyomo v.5.6.8 package [15, 16] and solve the resulting MINLPs using ANTIGONE, which is interfaced via the Pyomo-GAMS interface. We also tested other global MINLP solvers but the branch-and-cut based global optimization solver ANTIGONE turned out to be the most reliable and best performing one. All details of the algorithms inside ANTIGONE can be found in [25] and the references therein. In our computations, we use a relative optimality gap of 0.1 %. All other parameters are the default values of GAMS. The computations are executed on a computer with an Intel(R) Core(TM) i7-8550U processor with eight threads at 1.90 GHz and 16 GB RAM.

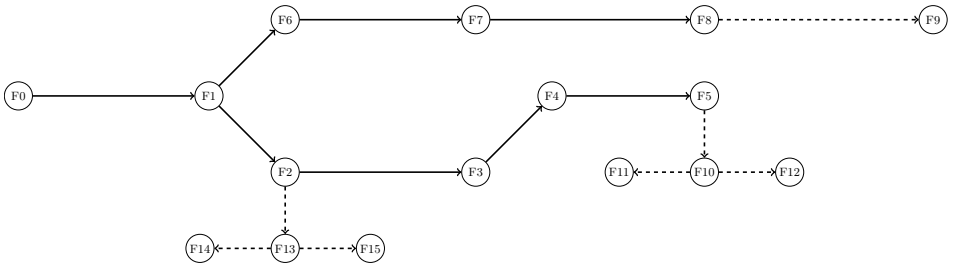

FIGURE 3. The tree-shaped forward-flow part of the network used in our case study. Solid lines are existing pipes and dashed lines correspond to candidate pipes. The node F0 is the depot.

TABLE 3. Left: Diameters of all pipes $a \in A_{\mathrm{ff}}$ in the forward-flow part of the network. Right: Average demands P_a for all consumers $a \in A_{\mathrm{c}}$.

Pipe	D (in mm)
(F0,F1)	107
(F1,F2)	107
(F1,F6)	107
(F2,F3)	83
(F2,F13)	70
(F3,F4)	83
(F4,F5)	70
(F5,F10)	70
(F6,F7)	83
(F7,F8)	70
(F8,F9)	70
(F10,F11)	70
(F10,F12)	70
(F13,F14)	70
(F13,F15)	70

Consumer	P (in kW)
(F2,B2)	200.00
(F3,B3)	600.00
(F5,B5)	150.00
(F6,B6)	666.66
(F8,B8)	200.00
(F9,B9)	183.33
(F11,B11)	183.33
(F12,B12)	183.33
(F14,B14)	183.33
(F15,B15)	183.33

4.2. **Test Cases.** We carry out our case study on the network shown in Figure 3. This network is based on the AROMA network used in [19], which we adapt and extend to our needs of computing optimal district heating network expansion decisions. In particular, the original network from the literature is modified so that it is tree-shaped, while keeping its other major characteristics. Table 3 (left) provides the diameters of all pipes in the forward-flow part of the network. The diameters of the corresponding pipes of the backward-flow part of the network are chosen identical.

As introduced previously, the parameter P_a represents the average demand of the consumer $a \in A_{\mathrm{c}}$; see Table 3 (right). The costs for connecting a new consumer are 100 000 €. The investment costs per meter of pipe as well as the mass flow's upper bound (both depending the chosen diameter) are given in Table 4 and taken from [28]. The costs C_a^{inv} in (19) thus correspond to the daily annuity of 100 000 € for consumers $a \in A_{\mathrm{c}}^{\mathrm{c}}$ and to the daily annuity of $C^{\mathrm{inv}} L_a$ for $a \in A_{\mathrm{ff}}^{\mathrm{c}} \cup A_{\mathrm{bf}}^{\mathrm{c}}$, where C^{inv} is given in Table 4.

We now discuss the operating costs of the depot. The price of waste incineration, of gas combustion, and the price of electricity (for increasing the pressure) are given

TABLE 4. Investment costs per pipe length and upper bounds on mass flow for all pipe diameters.

D_a (mm)	70	83	107
C^{inv} (€/m)	537.0	616.0	760.0
q_a^+ (kg s^{-1})	24.6	38.9	68.3

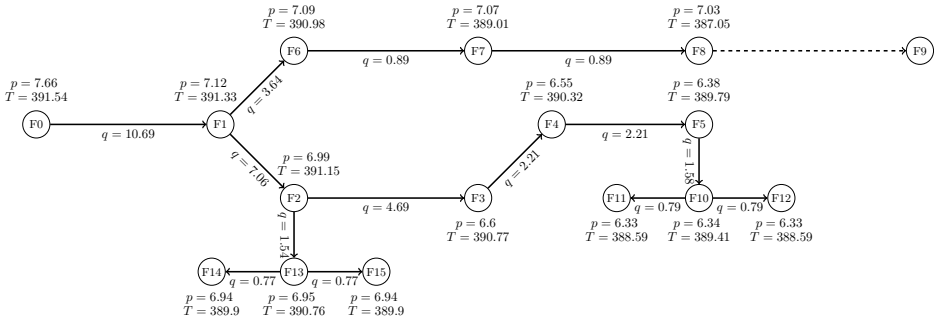

FIGURE 4. Illustration of the solution of Problem (20). Solid arcs represent existing and newly constructed candidate pipes whereas dashed arcs represent candidate pipes that are not built. The figure also provides parts of the physical solution (T in K and p in bar at nodes and q in kg s^{-1} on arcs).

by $C_{\text{w}} = 0$€/kWh, $C_{\text{g}} = 0.0415$€/kWh, and $C_{\text{p}} = 0.165$€/kWh, respectively. These cost data are also taken from [28]. A discount factor of 3 % per year is used to compute daily annuities. The energy selling price π, see (19), is based on [37]. We suppose that no upper bound on P_{g} and P_{p} exists. Contrarily, we impose a bound of 500 kW for P_{w}.

Finally, the approximation of the solution of the thermal energy equation is chosen to be of degree 2 and is computed separately for each pipe using a fine grid of 32 000 sample points on the domain imposed by the bounds on velocities and inlet temperatures; cf. Section 3. We also carried out an extensive computational sensitivity analysis to check if the results qualitatively change if the approximation is changed. To this end, we tested approximations obtained from a range between 8000 to 128 000 sample points. Since all results stayed very much the same, we do not discuss this sensitivity analysis in more detail.

4.3. **Discussion of the Results.** We start by discussing the results obtained for the parameterization of the problem discussed above. Figure 4 illustrates the solution, i.e., the solution of (20), in the forward-flow part of the network. The model contains 209 variables, thereof 19 being binary,[1] and 599 constraints. ANTIGONE takes 697 seconds to solve this problem. Note that, if we do not incorporate the additional valid binary inequalities derived in Section 2.7, ANTIGONE needs 5750 seconds to solve the problem. Thus, these inequalities lead to a speed-up factor larger than 8 on the tested instance. Besides Figure 4, Table 5 shows some relevant parameter values as part of the optimal solution, which we will later discuss in

[1]Note that we have 7 candidate pipes both in the forward and the backward flow network together with 5 binary variables for the potentially connected new consumers.

TABLE 5. Relevant parameters of the optimal solution.

Objective (€/day)	P_t (kW)	P_p (kW)	P_w (kW)	P_g (kW)	P_tl (kW)
−1380.02	2550.0	2.84	500.0	2149.87	99.87

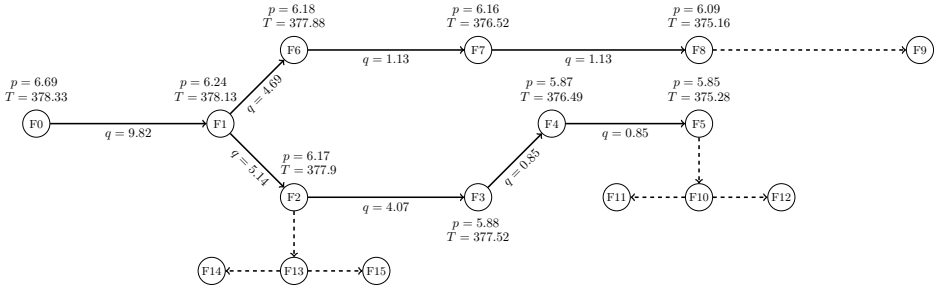

FIGURE 5. Solution of the optimization problem when $P_a = 150\,\mathrm{kW}$ for all $a \in A_\mathrm{c}^\mathrm{c}$.

detail. Besides the already defined ones, these are the total connected power load

$$P_\mathrm{t} := \sum_{a \in A_\mathrm{c}^\mathrm{e}} P_a + \sum_{a \in A_\mathrm{c}^\mathrm{c}} x_a P_a$$

and the thermal power losses P_tl in the system, which are given by

$$P_\mathrm{tl} := P_\mathrm{w} + P_\mathrm{g} - P_\mathrm{t}.$$

The solution has a rather high pressure at the depot's outlet node of 7.66 bar. This allows to increase the water's velocity in the network and, thus, the mass flow, which in turn allows to reduce temperature differences at the consumers; cf. (12a) or (12b). Thus, the optimal operation in this case is based on significantly increasing the pressure (from the stagnation pressure of 5 bar to 7.66 bar) at the rather high price $C_\mathrm{p} = 0.165\,€/\mathrm{kWh}$ (compared to the lower values for C_w and C_g). This increased outlet pressure at the depot leads to larger mass flows in the system. Thus, the required temperature differences at the consumers can be decreased. This, together with the resulting smaller thermal losses in the pipes, cf. (5), leads to comparably small overall thermal losses in the system, which are coped with by increasing the water temperature at the depot at the rather low prices for C_w and C_g.

4.3.1. *The Impact of Heat Demand on Expansion Decisions.* In Figure 5, we plot the solution for the forward flow network in case that all average consumer demands are reduced to 150 kW. It is clearly visible that this has a strong impact on the investment decision: no new consumer is connected to the network. Although being very important, the effect is rather obvious. Since the network operator mainly earns money by the consumption of connected households, significantly decreased demand leads to less income and thus the potentially new consumers are not worth to be connected.

4.3.2. *The Impact of the Distance Between the Existing Network and the New Consumer.* We measure the distance of a new consumer to the existing network in terms of the aggregated length of the required new pipes for connecting the new consumer. This distance influences how much the retailer pays to connect the consumer (at least) in two ways. First, the farther away a consumer is from the

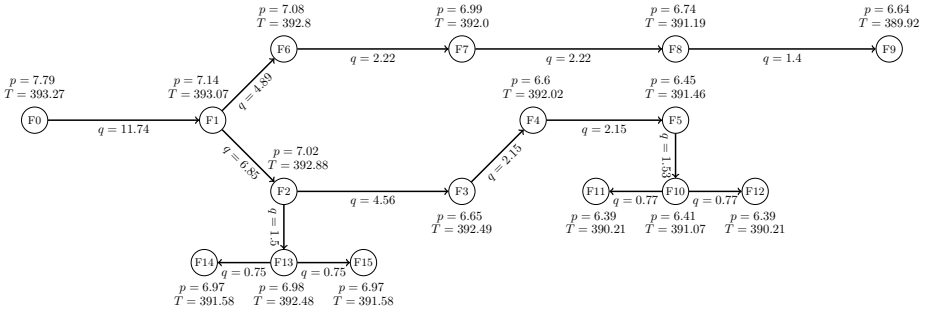

FIGURE 6. Solution of the optimization problem when $P_{(\mathrm{F9,B9})} = 350\,\mathrm{kW}$. The arc (F9,B9) is connected since its demand is high enough to overcome the pipe installation costs.

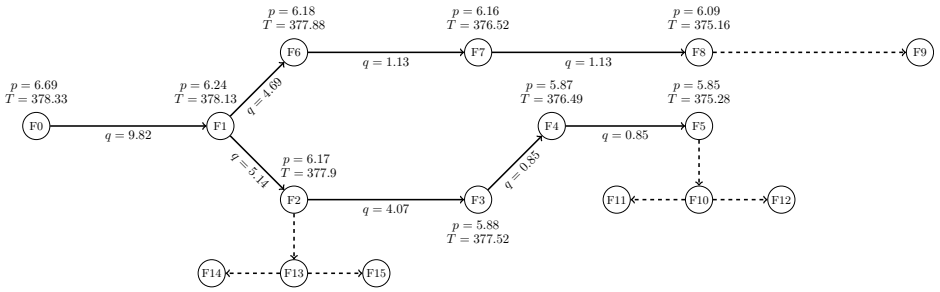

FIGURE 7. Solution of the optimization problem when U_a is set to $0.8\,\mathrm{W\,m^{-1}\,K^{-2}}$ for all a in A_c^c. No candidate consumers are connected since the additional thermal losses make it financially uninteresting.

existing network, the more needs to be paid to install the pipes that connect the new consumer to the network. This immediately influences the objective function; cf. the second term in (19). Second, larger distances lead to larger power and pressure losses in the system: The longer a pipe, the more thermal and pressure losses occur; see the solution (7) of the thermal energy equation and the momentum equation (4).

This explains why consumer (F9,B9) is not connected to the existing network. Indeed, we see that this consumer is located far away from the original network and thus induces high pipe costs and losses. If we, for instance, sufficiently increase the power demand or decrease the distance from this consumer to the existing network, it becomes financially worth to be connect this consumer as shown in Figure 6, which is obtained for $P_{(\mathrm{F9,B9})} = 350\,\mathrm{kW}$.

4.3.3. *The Impact of Power Losses.* Pressure and thermal losses represent the power loss in the network. Pressure losses (measured in power) correspond to P_p since this power is required to propel the water flow in the network. They represent approximately 0.1 % of the total power consumption in the solution (see Table 5) and thus do not have a significant importance for the expansion decisions. Thermal power losses P_tl represent 3.76 % of the total power consumption in the solution and, hence, are not negligible. To illustrate the importance of thermal losses, we increase the heat transfer coefficient U_a of all candidate pipes from 0.5 to $0.8\,\mathrm{W\,m^{-1}\,K^{-2}}$. The result is shown in Figure 7, where no candidate consumer is connected to the existing network at all. This shows that considering thermal power when making

expansion decisions is relevant, especially if different insulation techniques for water pipes are available.

5. Conclusion

In this paper, we presented a mixed-integer nonlinear optimization model for the district heating network expansion problem in case of tree-shaped networks. To the best of our knowledge, mixed-integer expansion decisions for district heating networks have not been combined before in the literature with a nonlinear modeling of thermal and hydraulic phenomena as accurate as in this paper. Whereas the accurate incorporation of the hydraulic effects is rather straightforward, the tackling of the energy equation modeling the thermal effects is more complicated. Here, we developed a novel polynomial approximation that is well tailored for optimization. Finally, in our case study we identified three main parameters that mainly govern the expansion decisions:

(i) The estimated average demand of the new consumer. Thus, it is important to have an accurate estimation of the future consumption of households. There are many papers in the literature that estimate the future heat demand of households; see, e.g., [39] for a case study in Sweden or [22, 27] for more general approaches for heat demand estimation. Even more relevant in our context, the authors of [30] try to predict heat demand based on consumer and building characteristics. Based on these predictions, they also estimate the profitability of connecting these new consumers by computing probability distributions to see if these candidate consumers have a high chance of being connected. However, the authors do not consider any network operation or expansion. In the light of the importance of the estimated demand, a highly reasonable topic of future research is to combine these two different branches of literature—namely heat future demand estimation and network expansion.

(ii) The distance of the candidate consumer to the existing network. Thus, one needs to accurately evaluate the pipe building costs and the chosen network layout if multiple consumers shall be connected. This aspect is, in principle, also covered in other papers on district heating networks such as [4] by also considering a price per length of the newly built pipes. However, we are, to the best of our knowledge, the first who measure these effects in the context of nonlinear and non-isothermal physics models.

(iii) Finally, the discussion of thermal power losses highlights the importance of a good pipe insulation. To the best of our knowledge, this aspect was not discussed in the literature before in this context.

To obtain a tractable model, we needed to simplify the problem. Note, however, that we still end up with a nonconvex mixed-integer nonlinear model, which is computationally very challenging. The most important assumption is that we restrict ourselves to the stationary case. Thus, we abstract from time-dependent, i.e. dynamic, effects of physics as well as from certain depot dynamics such as ramping constraints. Second, we only consider a single power-load scenario in the model. Incorporating multiple scenarios, for instance by using stochastic optimization, would allow for a better representation of future demands—and thus, most likely, for a better investment decision. However, this would put a significant additional computational burden. Third, we restricted ourselves to the case of tree-shaped networks to avoid complicating models for temperature mixing at the nodes of the network. Possible future work might also include the further exploitation of this tree-like structure to obtain more effective solution approaches for the problem discussed in this paper. If more general networks are considered, flow directions are

not known in advance and one needs mixing models that are nonsmooth and lead to the violation of standard constraint qualifications of nonlinear optimization; see, e.g., [19] for the details. Finally, we abstracted from also choosing the diameters of newly built pipes, which could also be incorporated in the model. All the mentioned aspects are out of the scope of this article but part of our future work.

Acknowledgments

The second author thanks the Deutsche Forschungsgemeinschaft for their support within projects A05 and B08 in the Sonderforschungsbereich/Transregio 154 "Mathematical Modelling, Simulation and Optimization using the Example of Gas Networks". Both authors acknowledge the support by the German Bundesministerium für Bildung und Forschung within the project "EiFer". Moreover, we are very grateful to all the colleagues within the EiFer consortium for many fruitful discussions on the topics of this paper and for providing the data.

References

[1] M. Ameri and Z. Besharati. "Optimal design and operation of district heating and cooling networks with CCHP systems in a residential complex." In: *Energy and Buildings* 110 (2016), pp. 135–148. DOI: 10.1016/j.enbuild.2015.10.050.

[2] A. Benonysson, B. Bøhm, and H. F. Ravn. "Operational optimization in a district heating system." In: *Energy Conversion and Management* 36.5 (1995), pp. 297–314. DOI: 10.1016/0196-8904(95)98895-T.

[3] M. Blommaert, R. Salenbien, and M. Baelmans. *An Adjoint Approach to Thermal Network Topology Optimization*. 2018. URL: https://lirias.kuleuven.be/retrieve/534620.

[4] C. Bordin, A. Gordini, and D. Vigo. "An optimization approach for district heating strategic network design." In: *European Journal of Operational Research* 252.1 (2016), pp. 296–307. DOI: 10.1016/j.ejor.2015.12.049.

[5] R. Borsche, M. Eimer, and N. Siedow. *A local time stepping method for district heating networks*. 2018. URL: https://kluedo.ub.uni-kl.de/frontdoor/deliver/index/docId/5140/file/district_heating.pdf.

[6] S. Bracco, G. Dentici, and S. Siri. "Economic and environmental optimization model for the design and the operation of a combined heat and power distributed generation system in an urban area." In: *Energy* 55 (2013), pp. 1014–1024. DOI: 10.1016/j.energy.2013.04.004.

[7] European Commission. *Communication from the Cimmission to the European Parliament, the European Council, the Council, the European Economic and Social Committe and the Committe of the Regions: The European Green Deal*. Accessed 2020-04-02. 2019. URL: https://ec.europa.eu/info/sites/info/files/european-green-deal-communication_en.pdf.

[8] T. Falke, S. Krengel, A.-K. Meinerzhagen, and A. Schnettler. "Multi-objective optimization and simulation model for the design of distributed energy systems." In: *Applied Energy* 184 (2016), pp. 1508–1516. DOI: 10.1016/j.apenergy.2016.03.044.

[9] A. Fügenschuh, B. Geißler, R. Gollmer, A. Morsi, M. E. Pfetsch, J. Rövekamp, M. Schmidt, K. Spreckelsen, and M. C. Steinbach. "Physical and technical fundamentals of gas networks." In: *Evaluating Gas Network Capacities*. Ed. by T. Koch, B. Hiller, M. E. Pfetsch, and L. Schewe. SIAM-MOS series on Optimization. SIAM, 2015. Chap. 2, pp. 17–44. DOI: 10.1137/1.9781611973693.ch2.

[10] B. Geißler, A. Morsi, L. Schewe, and M. Schmidt. "Solving Highly Detailed Gas Transport MINLPs: Block Separability and Penalty Alternating Direction Methods." In: *INFORMS Journal on Computing* 30.2 (2018), pp. 309–323. DOI: 10.1287/ijoc.2017.0780.

[11] E. Guelpa, G. Mutani, V. Todeschi, and V. Verda. "Reduction of CO2 emissions in urban areas through optimal expansion of existing district heating networks." In: *Journal of Cleaner Production* 204 (2018), pp. 117–129. DOI: 10.1016/j.jclepro.2018.08.272.

[12] C. Haikarainen, F. Pettersson, and H. Saxén. "A decomposition procedure for solving two-dimensional distributed energy system design problems." In: *Applied Thermal Engineering* 100 (2016), pp. 30–38. DOI: 10.1016/j.applthermaleng.2016.02.012.

[13] E. Hairer, S. P. Nørsett, and G. Wanner. *Solving ordinary differential equations I. Nonstiff problems*. Springer Series in Computational Mathematics, 1993. DOI: 10.1007/978-3-540-78862-1.

[14] F. M. Hante and M. Schmidt. "Complementarity-based nonlinear programming techniques for optimal mixing in gas networks." In: *EURO Journal on Computational Optimization* 7.3 (2019), pp. 299–323. DOI: 10.1007/s13675-019-00112-w.

[15] W. E. Hart, C. D. Laird, J.-P. Watson, D. L. Woodruff, G. A. Hackebeil, B. L. Nicholson, and J. D. Siirola. *Pyomo-optimization modeling in Python*. Springer, 2017. DOI: 10.1007/978-1-4614-3226-5.

[16] W. E. Hart, J.-P. Watson, and D. L. Woodruff. "Pyomo: modeling and solving mathematical programs in Python." In: *Mathematical Programming Computation* 3.3 (2011), pp. 219–260. DOI: 10.1007/s12532-011-0026-8.

[17] S.-A. Hauschild, N. Marheineke, V. Mehrmann, J. Mohring, A. M. Badlyan, M. Rein, and M. Schmidt. "Port-Hamiltonian modeling of district heating networks." In: *Progress in Differential Algebraic Equations II*. Differential-Albergaic Equations Forum. Springer, 2020.

[18] R. Köcher. "Beitrag zur Berechnung und Auslegung von Fernwärmenetzen." PhD thesis. Technische Universität Berlin, 2000. URL: http://nbn-resolving.de/urn:nbn:de:kobv:83-opus-821.

[19] R. Krug, V. Mehrmann, and M. Schmidt. "Nonlinear Optimization of District Heating Networks." In: *Optimization and Engineering* (2020). DOI: 10.1007/s11081-020-09549-0.

[20] X.-l. Li, L. Duanmu, and H.-w. Shu. "Optimal design of district heating and cooling pipe network of seawater-source heat pump." In: *Energy and Buildings* 42.1 (2010). International Conference on Building Energy and Environment (COBEE 2008), pp. 100–104. DOI: 10.1016/j.enbuild.2009.07.016.

[21] J. E. Marsden and A. J. Chorin. *A mathematical introduction to fluid mechanics*. Springer-Verlag, 1993. DOI: 10.1007/978-1-4684-0082-3.

[22] D. Meha, T. Novosel, and N. Duić. "Bottom-up and top-down heat demand mapping methods for small municipalities, case Gllogoc." In: *Energy* 199 (2020), p. 117429. DOI: https://doi.org/10.1016/j.energy.2020.117429. URL: http://www.sciencedirect.com/science/article/pii/S0360544220305363.

[23] T. Mertz, S. Serra, A. Henon, and J. Reneaume. "A MINLP optimization of the configuration and the design of a district heating network: study case on an existing site." In: *Energy Procedia* 116 (2017). 15th International Symposium on District Heating and Cooling, DHC15-2016, 4-7 September 2016, Seoul, South Korea, pp. 236–248. DOI: 10.1016/j.egypro.2017.05.071.

[24] T. Mertz, S. Serra, A. Henon, and J.-M. Reneaume. "A MINLP optimization of the configuration and the design of a district heating network: Academic study cases." In: *Energy* 117 (2016). The 28th International Conference on Efficiency, Cost, Optimization, Simulation and Environmental Impact of Energy Systems - ECOS 2015, pp. 450–464. DOI: 10.1016/j.energy.2016.07.106.

[25] R. Misener and C. A. Floudas. "ANTIGONE: Algorithms for coNTinuous / Integer Global Optimization of Nonlinear Equations." In: *Journal of Global Optimization* 59.2 (2014), pp. 503–526. DOI: 10.1007/s10898-014-0166-2.

[26] B. Morvaj, R. Evins, and J. Carmeliet. "Optimising urban energy systems: Simultaneous system sizing, operation and district heating network layout." In: *Energy* 116 (2016), pp. 619–636. DOI: 10.1016/j.energy.2016.09.139.

[27] T. Novosel, T. Pukšec, N. Duić, and J. Domac. "Heat demand mapping and district heating assessment in data-pour areas." In: *Renewable and Sustainable Energy Reviews* 131 (2020), p. 109987. DOI: https://doi.org/10.1016/j.rser.2020.109987. URL: http://www.sciencedirect.com/science/article/pii/S1364032120302781.

[28] T. Nussbaumer and S. Thalmann. "Influence of system design on heat distribution costs in district heating." In: *Energy* 101 (2016), pp. 496–505. DOI: 10.1016/j.energy.2016.02.062.

[29] A. Omu, R. Choudhary, and A. Boies. "Distributed energy resource system optimisation using mixed integer linear programming." In: *Energy Policy* 61 (2013), pp. 249–266. DOI: 10.1016/j.enpol.2013.05.009.

[30] M. Pagani, P. Maire, W. Korosec, N. Chokani, and R. Abhari. "District heat network extension to decarbonise building stock: A bottom-up agent-based approach." In: *Applied Energy* 272 (2020), p. 115177. DOI: https://doi.org/10.1016/j.apenergy.2020.115177. URL: http://www.sciencedirect.com/science/article/pii/S0306261920306899.

[31] M. Rein, J. Mohring, T. Damm, and A. Klar. "Parametric model order reduction for district heating networks." In: *PAMM* 18.1 (2018). DOI: 10.1002/pamm.201800192.

[32] G. Sandou, S. Font, S. Tebbani, A. Hiret, C. Mondon, S. Tebbani, A. Hiret, and C. Mondon. "Predictive Control of a Complex District Heating Network." In: *Proceedings of the 44th IEEE Conference on Decision and Control*. 2005, pp. 7372–7377. DOI: 10.1109/CDC.2005.1583351.

[33] M. Schmidt, M. C. Steinbach, and B. M. Willert. "High detail stationary optimization models for gas networks." In: *Optimization and Engineering* 16.1 (2015), pp. 131–164. DOI: 10.1007/s11081-014-9246-x.

[34] M. Schmidt, M. C. Steinbach, and B. M. Willert. "High detail stationary optimization models for gas networks: validation and results." In: *Optimization and Engineering* 17.2 (2016), pp. 437–472. DOI: 10.1007/s11081-015-9300-3.

[35] M. Schmidt, M. C. Steinbach, and B. M. Willert. "The precise NLP model." In: *Evaluating Gas Network Capacities*. Ed. by T. Koch, B. Hiller, M. E. Pfetsch, and L. Schewe. SIAM-MOS series on Optimization. SIAM, 2015. Chap. 10, pp. 181–210. DOI: 10.1137/1.9781611973693.ch10.

[36] J. Söderman. "Optimisation of structure and operation of district cooling networks in urban regions." In: *Applied Thermal Engineering* 27.16 (2007). Selected Papers from the 9th Conference on Process Integration, Modelling and Optimisation for Energy Saving and Pollution Reduction – PRES2006, pp. 2665–2676. DOI: 10.1016/j.applthermaleng.2007.05.004.

[37] TWL. *Preise für Fernwärme*. Last accessed 2020-03-25. 2020. URL: https://www.twl.de/privatkunden/meine-energie/fernwaerme/.

[38] F. Verrilli, S. Srinivasan, G. Gambino, M. Canelli, M. Himanka, C. Del Vecchio, M. Sasso, and L. Glielmo. "Model Predictive Control-Based Optimal Operations of District Heating System With Thermal Energy Storage and Flexible Loads." In: *IEEE Transactions on Automation Science and Engineering* 14.2 (2017), pp. 547–557. DOI: 10.1109/TASE.2016.2618948.

[39] S. Werner. "District heating and cooling in Sweden." In: *Energy* 126 (2017), pp. 419–429. DOI: https://doi.org/10.1016/j.energy.2017.03.052. URL: http://www.sciencedirect.com/science/article/pii/S0360544217304140.

Appendix A. Proof of Lemma 1

Two cases are considered for solving the ODE. First, we consider $v_a = 0$. Then, (5) reduces to

$$\frac{4U_a}{c_\mathrm{p}\rho D_a}(T_a(x) - T_\mathrm{soil}) = 0, \quad x \in [0, L_a].$$

This obviously leads to the first case in (6).

Next, we consider the case $v_a > 0$. In this case, (5) can be rewritten as

$$\frac{\mathrm{d}T_a}{\mathrm{d}x}(x) + \frac{4U_a}{c_\mathrm{p}\rho D_a v_a}T_a(x) = \frac{4U_a}{c_\mathrm{p}\rho D_a v_a}T_\mathrm{soil}, \quad x \in [0, L_a].$$

We know from classical ODE theory, see, e.g., [13], that the first-order ODE of the form

$$\frac{\mathrm{d}y(x)}{\mathrm{d}x} + ay(x) = b,$$

with constants a and b has the solution

$$y(x) = Ce^{-ax} + \frac{b}{a},$$

with C being another constant. This then allows to derive the second case of (6).

To prove continuity and since both cases in (6) are composed of continuous functions it suffices to see that

$$\lim_{v_a \to 0} T_a(x; v_a) = T_\mathrm{soil} = T_a(x; 0)$$

for all $x \in [0, L_a]$. This concludes the proof.

(M. Roland, M. Schmidt) [1]Trier University, Department of Mathematics, Universitätsring 15, 54296 Trier, Germany

Email address: roland@uni-trier.de, martin.schmidt@uni-trier.de